

Mono- and Dinuclear Ruthenium(II) Complexes of 2,6-Di(pyrazol-3-yl)pyridines: Deprotonation, Functionalization, and Supramolecular Association

Jerzy Zadykowicz and Pierre G. Potvin*

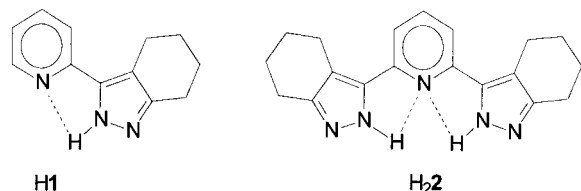
Department of Chemistry, York University, 4700 Keele Street, Toronto, ON, Canada M3J 1P3

Received July 15, 1998

A number of Ru(II) complexes, both homo- and heteroleptic, of variously N-substituted 2,6-di(4,5,6,7-tetrahydroindazol-3-yl)pyridines have been prepared from the free ligands or by N-alkylations of Ru-bound, *N*-H-bearing ligands. Carboxyl-bearing complexes were prepared by hydrolysis of the corresponding esterified complexes. All were characterized by elemental analysis and by their NMR, FAB-MS, and UV–visible spectra, and a selection was additionally submitted to cyclic voltammetry. The fully substituted complexes showed MLCT bands in the 414–424 nm range and $E_{1/2}^{3+/2+}$ values in the +0.83–0.98 V range. Comparisons with data from related complexes are discussed. A heteroleptic dinuclear species was prepared from a CH₂-linked bis(tridentate) and found to consist of the *like* (chiral racemic) diastereomer. It showed a single MLCT band at 416 nm and a single Ru^{3+/2+} couple at +0.98 V. In the case of *N*-H-bearing complexes, deprotonation caused the appearance of a less energetic MLCT band and multiple CV waves at lower oxidation potentials. There was also evidence of loss of H[•] at negative potentials. A supramolecular 2:1 salt formed between the deprotonated form of the homoleptic complex of 2,6-di(1-(4-carboxyphenyl)-4,5,6,7-tetrahydroindazol-3-yl)pyridine and methyl viologen dication.

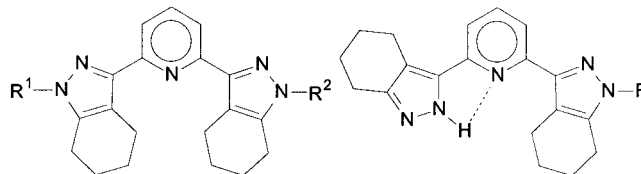
Introduction

Ru^{II} complexes of bipyridine (bpy) and terpyridine have attracted much attention due to their potential application as photocatalysts.¹ This has stimulated work with other ligands composed of combinations of azines and azoles,² including the π -rich pyrazolopyridines and bispyrazolopyridines. In previous work, we have reported the preparation of the 3'(C'),2-linked 2-(tetrahydroindazol-3-yl)pyridine, **H1**, from commercially available materials by a short route and in good yields.³ Ru^{II} complexes of **H1** and of several of its 1(N)-substituted derivatives have been prepared and studied in detail.^{4,5} Compared with bpy in Ru(bpy)₃²⁺, these showed higher $d\pi$ and π^* levels, with E_L parameters⁶ of 0.21–0.22 V,⁴ but the ligand remained flat in crystals.⁵



We wished to similarly examine complexes of the tridentate analogue of **H1**, the symmetrical 2,6-di(4,5,6,7-tetrahydroindazol-3-yl)-

pyridine **H22**, which is also easily prepared.^{7,8} Like **H1** but unlike the 1'(N'),2-linkage isomers,^{9,10} **H22** is amenable to modification at the 1(N)-H sites. This facility has enabled us to prepare a variety of substituted tridentates^{8,11,12} and a ditopic bis(tridentate)¹¹ as well as novel pentadentate and macrocyclic⁷ ligands. We have also demonstrated how these ligands can bind alkali metal ions, Fe(III), Ru(II),^{7,11,13} Zn(II),¹¹ and Co(II).^{12,14} The liposolubilities of **H1** and **H22** and their derivatives and complexes have proven to be synthetically very advantageous.



- 3** R¹ = R² = Me
5 R¹ = R² = C₆H₄-4-COOEt
7 R¹ = R² = Et
8 R¹ = R² = CH₂Ph
9 R¹ = R² = CH₂C₆H₄-4-COOMe
10 R¹ = R² = CH₂COOEt
11 R¹ = Me R² = CH₂Br
H213 R¹ = R² = C₆H₄-4-COOH
H214 R¹ = R² = CH₂C₆H₄-4-COOH
H215 R¹ = R² = CH₂COOH

We now report on the preparation and characterization of Ru^{II} complexes of a number of derivatives of **H22**, including a dinuclear species, on the novel alkylation of *N*-H-bearing complexes and on supramolecular binding of methyl viologen by a COOH-bearing complex.

* Corresponding author. Tel.: (416) 736-2100, ext. 66140. Fax: (416) 736-5936. E-mail: pspotvin@yorku.ca.

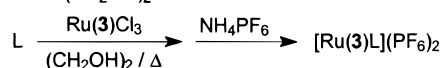
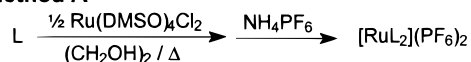
- (1) Sauvage, J.-P.; Collin, J.-P.; Chambron, J.-C.; Guillerez, S.; Coudret, C.; Balzani, V.; Barigelli, F.; De Cola, L.; Flamigni, L. *Chem. Rev.* **1994**, *94*, 993.
 (2) E. C. Constable, *Adv. Inorg. Chem. Radiochem.* **1986**, *30*, 69.
 (3) Luo, Y.; Potvin, P. G. *J. Org. Chem.* **1994**, *59*, 1761.
 (4) Luo, Y.; Potvin, P. G.; Tse, Y.-H.; Lever, A. B. P. *Inorg. Chem.* **1996**, *35*, 5445.
 (5) Luo, Y.; Potvin, P. G. *J. Coord. Chem.* **1999**, *46*, 319.
 (6) Lever, A. B. P. *Inorg. Chem.* **1990**, *29*, 1271; **1991**, *30*, 1980. Masui, H.; Lever, A. B. P. *Inorg. Chem.* **1993**, *32*, 2199.

(7) Dash, R.; Potvin, P. G. *Can. J. Chem.* **1992**, *70*, 2249.

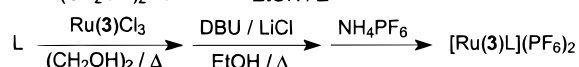
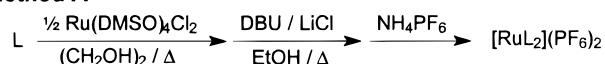
(8) van der Valk, P.; Potvin, P. G. *J. Org. Chem.* **1994**, *59*, 1766.

Scheme 1

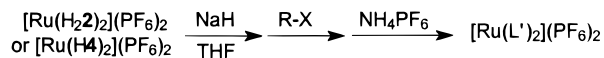
Method A



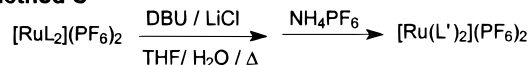
Method A'



Method B



Method C



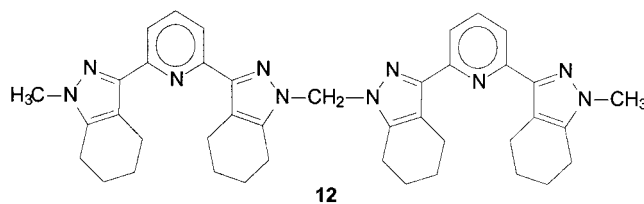
Results and Discussion

Synthesis. Although the reaction of Ru(DMSO)₄Cl₂¹⁵ with the unsubstituted H₂2 in EtOH at reflux⁷ was facile, reactions with the disubstituted derivatives, such as **3**, required higher temperatures (Scheme 1). Ethylene glycol at or near the boiling point (method A) gave satisfactory results. Reactions in DMF or DMPU or reactions with RuCl₃ were incomplete, and reactions in DMSO did not proceed at all with hindered ligands. The less hindered, monosubstituted derivatives, such as H₄, reacted well in ethylene glycol even at lower temperatures. Method A was also useful for the preparation of heteroleptic complexes. Thus, RuCl₃ was converted to Ru(3)Cl₃ by a modified literature procedure,¹⁶ then to [Ru(3)(H₄)](PF₆)₂ by method A. However, ligands bearing ester groups (**5** and H₆) suffered extensive transesterification, giving a mixture of products that necessitated a retro-transesterification step (DBU/LiCl/EtOH)¹⁷ in the workup (method A'). The heteroleptic [Ru(3)(5)](PF₆)₂ was similarly prepared from Ru(3)Cl₃.

When complexes bearing unsubstituted *N*-H sites were exposed to bases of various potencies (NaOH, CsCO₃, DBU, NaH), there was an immediate color change from red to green, accompanied by a shift of the MLCT bands toward the red. In most cases, this was entirely reversed upon re-acidification. On alumina TLC plates, this was spontaneous and useful in distinguishing partly *N*-substituted complexes from fully substituted ones. In air, the H₂O-soluble [Ru(H₂2)₂]Cl₂⁷ produced

the H₂O-insoluble but CHCl₃-soluble Ru^{III} species [Ru(2)(H₂)], which was blue (λ_{max} 538 nm), NMR-silent, and analytically halide-free.¹³ Although the deprotonated forms of *N*-H-bearing complexes are strongly stabilized by complexation, they remained moderately nucleophilic as they readily reacted with alkylating agents to generate new red products. Thus, [Ru(H₂2)₂](PF₆)₂ was treated with NaH in THF, followed by excess CH₃I (method B), to afford [Ru(3)₂](PF₆)₂ identical with material prepared from free **3** by method A.¹⁸ We also verified that the partially methylated complexes [Ru(H₄)₂](PF₆)₂ and Ru(3)(H₄)](PF₆)₂ also produced the fully methylated [Ru(3)₂](PF₆)₂ by this method. To our knowledge, these are the first instances of such modifications on complexed ligands, although the regioselective functionalizations of free H₂2 reported earlier^{8,11} depended on transient coordination to Na⁺ or K⁺. This reaction enabled us to prepare a number of new derivatives of [Ru(H₂2)₂](PF₆)₂ bearing ethyl, benzyl, and esterified acetic acid or *p*-toluic acid side chains. This complexation-alkylation route has certain advantages over the corresponding alkylation-complexation route in that the complexation step is much easier and more convenient with less congested ligands, there is no risk of producing regiomers and there is no risk of transesterification when ester groups are present. The overall yields were higher as well. For instance, ligands **9**¹¹ and **10**⁸ were known and could also produce [RuL₂]²⁺ complexes by method A, albeit in lower yields than by method B. However, the [Ru(7)₂](PF₆)₂ and [Ru(8)₂](PF₆)₂ produced by method B are complexes of ligands that are unknown in their free states. [Ru(H₆)₂](PF₆)₂ was also similarly methylated on a small scale to help resolve overlaps in the NMR spectra.

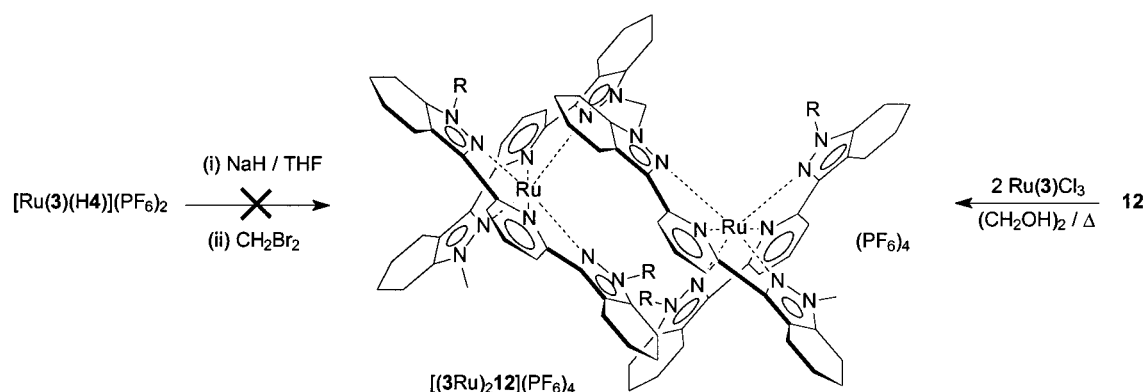
A logical application of this complexation-alkylation process is to assemble oligonuclear species. We had earlier¹¹ identified -CH₂- bridges as desirably short linkages between octahedral centers that would favor helicity, i.e. the formation of *like* (chiral racemic) diastereomeric forms of any two-metal fragment of a chain, as opposed to *unlike* (mesoid) forms. We therefore attempted alkylations of *N*-H-bearing complexes with CH₂Br₂. Unfortunately, the reaction of [Ru(H₄)₂](PF₆)₂ with 1 equiv of CH₂Br₂ failed to provide the expected, doubly stranded, binuclear *helicate*, nor did [Ru(3)(H₄)](PF₆)₂ produce the desired singly stranded binuclear complex (Scheme 2). Both reactions instead gave complicated mixtures and similar results were obtained with CH₂I₂. NMR analysis of the product mixtures led us to suspect that CH₂Br groups were present. Indeed, the reaction of [Ru(H₄)₂](PF₆)₂ with an excess of CH₂Br₂ produced the novel bis(bromomethylated) [Ru(11)₂](PF₆)₂. Although this and the putative *mono*(bromomethylated) intermediate both possess leaving groups, their displacements by the deprotonated species [Ru(4)₂]⁰ or [Ru(4)(11)]⁺ were perhaps too sterically hindered. The same can be said of the intermediates in the earlier reactions with [Ru(H₄)₂](PF₆)₂ and [Ru(3)(H₄)](PF₆)₂. There was evidently no anchimeric assistance of the second X⁻ displacements at the complexes' -CH₂X side chains, in contrast to reactions of free H₄, which led cleanly to the ditopic ligand **12**¹¹ even with excess CH₂X₂ because of that assistance. Instead,



(18) Zadykowicz, J.; Potvin, P. G. *J. Coord. Chem.* **1999**, *47*, 395.

- (9) Saha, N.; Kar, S. K. *J. Inorg. Nucl. Chem.* **1977**, *39*, 1236. Watson, A. A.; House, D. A.; Steel, P. J. *J. Org. Chem.* **1991**, *56*, 4072. Chabert, N.; Jacquet, L.; Marzin, C.; Tarrago, G. *New J. Chem.* **1995**, *19*, 443. Steel, P. J.; Constable, E. C. *J. Chem. Soc., Dalton Trans.* **1990**, 1389. Lecloux, D. D.; Tolman, W. B. *J. Am. Chem. Soc.* **1993**, *115*, 1153. Jameson, D. L.; Blaho, J. K.; Kruger, K. T.; Goldsby, K. A. *Inorg. Chem.* **1989**, *28*, 4312. Jameson, D. L.; Goldsby, K. A. *J. Org. Chem.* **1990**, *56*, 4072.
- (10) Downard, A. J.; Honey, G. E.; Steel, P. J. *Inorg. Chem.* **1991**, *30*, 3733.
- (11) Zadykowicz, J.; Potvin, P. G. *J. Org. Chem.* **1998**, *63*, 235.
- (12) Jairam, R.; Lau, K.; Adorante, J.; Potvin, P. G. *Can. J. Chem.* **1999**, submitted.
- (13) Dash, R. M.Sc. Thesis, York University, 1991.
- (14) Jairam, R. M.Sc. Thesis, York University, 1991.
- (15) Evans, I. P.; Spencer, A.; Wilkinson, G. *J. Chem. Soc., Dalton Trans.* **1973**, 204.
- (16) Hadda, T. B.; Le Bozec, H. *Inorg. Chim. Acta* **1993**, *204*, 103.
- (17) Seebach, D.; Thaler, A.; Blaser, D.; Ko, S. Y. *Helv. Chim. Acta* **1991**, *74*, 1102.

Scheme 2



the binuclear species $[(3\text{Ru})_2(12)](\text{PF}_6)_4$ was obtained after mild heating of **12** with $\text{Ru}(3)\text{Cl}_3$ in ethylene glycol. Higher temperatures caused extensive fragmentation to produce $[\text{Ru}(3)(\text{H}4)]^{2+}$, quite probably by anchimerically assisted expulsion of $[\text{Ru}(3)(4)]^+$ from a mononuclear intermediate. FAB-MS of $[(3\text{Ru})_2(12)](\text{PF}_6)_4$ showed evidence of a similar fragmentation, with a peak at m/z 780 corresponding to $[\text{Ru}(3)(4)]^+$.

Carboxy-functionalized complexes were also of interest to us, but they were unfortunately not directly accessible from HOOC-bearing ligands¹¹ by method A, giving instead brown-green mixtures even when reacting under an Ar blanket. Instead, the acidic complexes $[\text{Ru}(\text{H}_2\mathbf{13})_2](\text{PF}_6)_2$, $[\text{Ru}(\text{H}_2\mathbf{14})_2](\text{PF}_6)_2$, and $[\text{Ru}(\text{H}_2\mathbf{15})_2](\text{PF}_6)_2$ were generated by hydrolyses (DBU/LiCl/THF/H₂O)¹⁷ of the corresponding ester-bearing complexes $[\text{Ru}(\mathbf{5})_2](\text{PF}_6)_2$, $[\text{Ru}(\mathbf{9})_2](\text{PF}_6)_2$, and $[\text{Ru}(\mathbf{10})_2](\text{PF}_6)_2$, respectively (method C).

Although many of the complexes studied here were isolable as their Cl^- salts—some were partly characterized as such—the PF_6^- salts were preferred for their greater liposolubilities and chromatographic separabilities. The complexes were characterized by elemental analysis and FAB-MS, as well as ¹H and ¹³C NMR (see below). In FAB-MS, the ion of highest mass usually resulted from the loss of one counteranion. Lower mass peaks corresponded to further anion loss, and to doubly charged ions. The HOOC-bearing complexes were the most troublesome to purify and characterize. FAB-MS was only successful in glycerol/thioglycerol matrixes. Repeated microanalyses of recrystallized $[\text{Ru}(\text{H}_2\mathbf{13})_2](\text{PF}_6)_2$ and $[\text{Ru}(\text{H}_2\mathbf{14})_2](\text{PF}_6)_2$ failed to give the expected results, suggesting instead a partial loss of the elements of HPF_6 during recrystallization.

NMR Spectroscopy and Structure. The ¹H NMR spectra fully supported the formulations and structures of the complexes described herein. In our experience with the in situ binding of Na^+ , Zn^{II} , Ti^{IV} , or D^+ by our tridentates,^{8,11} as well as with Ru^{II} complexes of the bidentate analogues,⁴ a comparison of the relative positioning of the pyridine signals from the complexes with that from the free ligands can reveal the regiochemistry of N-substitution and can confirm the formation of a complex through the occurrence of conformational changes about the inter-ring bonds. Thus, *out* N-substitution (i.e. at position 1 according to the indazole numbering) of an unsubstituted (*N*-H-bearing) tetrahydroindazole moiety is signaled by an inversion of the positioning of the pyridine H-3/5 doublet(s) with respect to the H-4 triplet (or doublet of doublets), a relative positioning which reverts to the original situation upon metal or proton binding. There is no such change upon complexation of an *N*-H-bearing moiety. An unsubstituted tetrahydroindazole moiety is held in a *syn* conformation with respect to the pyridine ring by virtue of H-bonding involving the pyridine N and the

in regiomer (i.e. the *2H* tautomer) of the tetrahydroindazole portion, whereas an *out*-substituted moiety prefers an *anti* conformation which reverts to the *syn* conformation upon complexation. The causes of these chemical shift changes have been discussed earlier, and our interpretations have recently been confirmed by crystallography.^{5,18}

In the present work, the complexation of our disubstituted ligands resulted in a change in the pyridine signal pattern entirely consistent with the binding of the metal at all three available nitrogens of an *out, out*-disubstituted ligand in its *syn, syn* conformer. The complexation of a monosubstituted ligand caused a shift in pattern that was similarly consistent with a change from a *syn, anti* conformation to a *syn, syn* one, with a necessary migration of the N-2-H to produce the 1-tautomer. Subsequent alkylation caused no further change in the signal pattern, but only *out* substitution is possible if the *N*-H-bearing ligand is also bound at its three available nitrogens. That this was indeed so was indicated by the increase in acidity of *N*-H-bearing ligands upon complexation. The formation of the same tetramethylated complex $[\text{Ru}(3)_2]^{2+}$ from free **3** as by alkylation of complexed **H4** also confirms this scenario. The crystal structure of $[\text{Ru}(3)_2]\text{Cl}_2$ has recently been obtained¹⁸ and it confirmed the expected *pseudo*-octahedral coordination, as well as the regiochemistry of substitution and the ring orientations.

¹H NMR spectroscopy was also useful in specifying the structure of the binuclear complex. As expected, the ¹H NMR spectrum of $[(3\text{Ru})_2(12)](\text{PF}_6)_4$ signaled the *like*, helical diastereomer: There were only two sets of pyridine signals in 1:1 ratio, indicating equivalent units of **4** within the ditopic **12**. There were three CH₃ singlets in 1:1:1 ratio, a situation that implies a symmetric unit of **12** and 2 equiv of an unsymmetric **3** moiety. The environment of each **3** is therefore chiral. All CH₃ singlets were strongly shifted upfield, an expected effect of the ring currents of perpendicular ligands (see Scheme 2). The CH₂ signal, also shifted upfield for the same reason, appeared as a singlet, confirming that the two metal centers had the same chirality. Diastereotopicity would have been expected in the *unlike* form. None was found in Zn^{2+} or Na^+ complexes either¹¹ but, in those cases, a rapid interchange between enantiomorphs via free rotation about the N-CH₂ bonds may have occurred. In the present case, the lack of symmetry in the dimethylated ligand **3** proved that there was no exchange of the metal chirality, presumably because of strong steric hindrance to such N-CH₂ rotation.

An unexpected case of diastereotopicity was observed with the bis(bromomethyl) complex $[\text{Ru}(\mathbf{11})_2](\text{PF}_6)_2$. In concentrated solution (35 mg/mL), the CH₂Br groups were diastereotopic and gave a pair of coupled doublets ($J = 11$ Hz) but gave a singlet in more dilute solution. We postulate that a more intimate

Table 1. UV–Vis Absorption Maxima (nm) by [Ru(L)₂]²⁺ in CH₃CN

L	L $\pi \rightarrow \pi^*$	MLCT [$\epsilon \times 10^{-3} \text{ M}^{-1} \text{ cm}^{-1}$]
H ₂ 2	248–314	414 [25.8]
3	244–324	418 [16.5]
5	272–320	424 [20.0]
H6	274–322	420 [13.8]
6 ⁻	278–350	446 [10.5]
7	244–324	416 [16.2]
8	244–326	416 [17.4]
9	208–328	416 [18.1]
10	250–320	416 [17.0]
13	272–330	422 [20.8] ^a
14	208–328	416 [18.4] ^a
15	250–320	418 [14.7] ^a

^a In methanol.

association of the PF₆⁻ counterions with the complex was occurring in the concentrated solution and that this reduced the mobility of the CH₂Br side chains. A similar phenomenon was reported for a terpyridine Ru complex bearing –CH₂N side chains: the CH₂ groups showed ¹H NMR singlets, as expected for freely rotating side chains, but these produced an AB pattern when in the presence of dicarboxylate salts that were engaged in H bonding to the side chains.¹⁹

Electronic Spectra. In general agreement with the spectra of Ru polypyridine²⁰ and pyrazolylpyridine⁴ complexes, the complexes exhibited two major absorptions (Table 1), one in the 210–330 nm range assigned to ligand-centered ($\pi \rightarrow \pi^*$) transitions and the other in the 416–424 nm range assigned to metal-to-ligand charge transfer (MLCT) ($d \rightarrow \pi^*$) transitions. The MLCT positions lie intermediate between that with [Ru(tpy)₂]²⁺ (476 nm)²¹ and that of the complex of the N-linked analogue 2,6-di(pyrazol-1-yl)pyridine (dpp) (377 nm).¹⁰ There is a weak substituent effect on the MLCT positions: complexes with aromatic substituents have slightly lower energy MLCT bands (420–424 nm) than do those with alkyl substituents (416–418 nm), entirely in accord with the expectation that electron-withdrawing groups will lower the ligand π^* levels.²⁰ The modesty of the effect is probably due to an orientation orthogonal to the pyrazole plane, as was found in our bidentate analogue.⁴ Not surprisingly, the binuclear [(3Ru)₂12]⁴⁺ showed a single but very intense MLCT band at 416 nm (ϵ 28 900 M⁻¹ cm⁻¹) in CH₃OH.

In the presence of base, both the $\pi \rightarrow \pi^*$ and MLCT bands of [Ru(H6)₂](PF₆)₂ shifted toward the red. In agreement with previous descriptions of similar phenomena with N-H-bearing complexes,^{22,23} the lower energy band is likely due to deprotonated form(s) in which 6⁻ has increased π -donor properties. Similarly, the treatment of a CH₃CN solution of [Ru(H₂2)₂](PF₆)₂ with aliquots of Et₃N (up to 5 equiv) caused the disappearance of the 414 nm band and the appearance of a new, red-shifted MLCT absorption at 434 nm.

Electrochemistry. Cyclic voltammetry (CV) plots of fully substituted complexes (Table 2) each revealed a Ru^{3+/2+} wave

Table 2. Half-Wave Potentials (V vs SCE),^a Estimated HOMO–LUMO Gaps ΔE (V), and E_L ligand parameters (V)

complex	$E_{1/2}^{3+/2+}$	$E_{1/2}^{2+/+}$	ΔE	E_L
[Ru(3) ₂] ²⁺	+0.83	-1.66 ^b	2.49	0.18
[Ru(5) ₂] ²⁺	+0.93	-1.52	2.45	0.20
[Ru(9) ₂] ²⁺	+0.96	-1.53 ^b	2.49	0.20
[(3Ru) ₂ 12] ⁴⁺	+0.98	-1.50 ^b	2.48	0.23 ^c
[Ru(3)(H4)] ²⁺	+0.71	-1.1 ^{b,d}		0.14 ^e
[Ru(3)(4)] ⁺	+0.37			0.03 ^f
[Ru(H ₂ 2) ₂] ²⁺ ^g	+0.63			0.15
[Ru(tpy) ₂] ²⁺ ^h	+1.27	-1.27	2.54	0.26
[Ru(dpp) ₂] ²⁺ ⁱ	+1.25	-1.66 ^d	2.91	0.25
[Ru(H1) ₃] ²⁺ ^j	+0.93			0.21
[Ru(Ar1) ₃] ²⁺ ^{j,k}	+1.12	-1.66	2.78	0.22

^a Reversible or quasi-reversible waves scanned at 100 mV s⁻¹ in CH₂Cl₂ containing 0.1 M ⁿBu₄NPF₆ at 20 ± 1 °C. ^b Estimated. ^c For 12. ^d Irreversible. ^e For H4. ^f For 4⁻. ^g In DMSO. Several other waves were also present (see text). ^h Reference 24. ⁱ bpp is 2,6-di(1-pyrazolyl)pyridine from ref 10. ^j Reference 4. ^k Ar1 is 1-(4-ethoxycarbonylphenyl)-3-(2-pyridyl)-4,5,6,7-tetrahydroindazole.

and a reversible or quasi-reversible reduction wave and can be compared with results from Ru^{II} complexes of the N,N'-linkage isomer,¹⁰ of tpy²⁴ and of the bidentate analogues⁴ of H₂2 (H1) and of 5 (Ar1). The nature of the N-substituents exerted a minor influence but a more important one than had been seen with the bidentate analogues.⁴ The Ru^{3+/2+} waves were at less positive values than with the bidentate analogues which, in turn, were less positive than with [Ru(tpy)₂]^{3+/2+}, reflecting the pyridine content in each case and signaling higher t_{2g} levels with increasing pyrazole content. As with the bidentate analogues in relation to [Ru(bpy)₃]²⁺, our tridentate complexes were reduced at more negative potentials than was [Ru(tpy)₂]²⁺, indicating higher ligand π^* levels and poorer π -accepting properties due to the π -rich pyrazole rings. The parallel increases in both metal-centered HOMO and ligand-centered LUMO resulted in the spreads between oxidation and reduction waves ($\Delta E = E_{1/2}^{2+/+} - E_{1/2}^{3+/2+}$) in Table 2 that were a little smaller than with [Ru(tpy)₂]²⁺, which is not consistent with the MLCT bands lying at somewhat higher energy. In comparison, the N-linked analogue [Ru(dpp)₂]²⁺ was oxidized at a potential comparable to that of [Ru(tpy)₂]²⁺ but it was reduced at a more negative potential, such that its ΔE value was significantly larger.¹⁰ This indicates a comparable t_{2g} level but a higher ligand π^* level than in [Ru(tpy)₂]²⁺, and is consistent with a significantly higher-energy MLCT band (Table 1). In fact, our complexes do not follow the linear relationship between MLCT energies and ΔE constituted by [Ru(tpy)₂]²⁺, [Ru(dpp)₂]²⁺, and the bidentate complexes [Ru(bpy)₃]²⁺ and [Ru(Ar1)₃]²⁺. It appears that our C-linked pyrazolylpyridines are comparable π donors but better σ donors than is the N-linked variety. This is consistent with conclusions drawn from crystal structure studies.^{5,18}

The known Lever ligand electrochemical parameters⁶ E_L and those calculated for the new ligands are included in Table 2. In view of the E_L values of mono(pyrazolyl)pyridine analogues (e.g. H1) that are lower than those of the polypyridines, our bis(pyrazolyl)pyridines have understandably even lower values, which are further decreased by electron-donating or H groups or by deprotonation. In contrast, the N,C-linkage isomer dpp has a higher E_L value.

[Ru(3)(H4)](PF₆)₂ in CH₂Cl₂ produced a major oxidation wave at +0.71 V vs SCE accompanied by a more minor wave

- (19) Goodman, M. S.; Jubian, V.; Hamilton, A. D. *Tetrahed. Lett.* **1995**, 2551.
 (20) Juris, A.; Balzani, V.; Barigelli, F.; Campagna, S.; Belser, P.; von Zalewsky, A. *Coord. Chem. Rev.* **1988**, 84, 85.
 (21) Hecker, C. R.; Gushurst, A. K. I.; McMillin, D. R. *Inorg. Chem.* **1991**, 30, 538.
 (22) Hage, R.; Prins, R.; Haasnoot, J. G.; Reedijk, J. *J. Chem. Soc., Dalton Trans.* **1987**, 1389.
 (23) Sullivan, B. P.; Salmon, D. J.; Meyer, T. J.; Peedin, J. *Inorg. Chem.* **1978**, 17, 3334; Belser, P.; von Zalewsky, A. *Helv. Chim. Acta* **1980**, 63, 1675.

- (24) Morris, D. E.; Hanck, K. W.; DeArmond, M. K. *J. Electroanal. Chem.* **1983**, 149, 115.

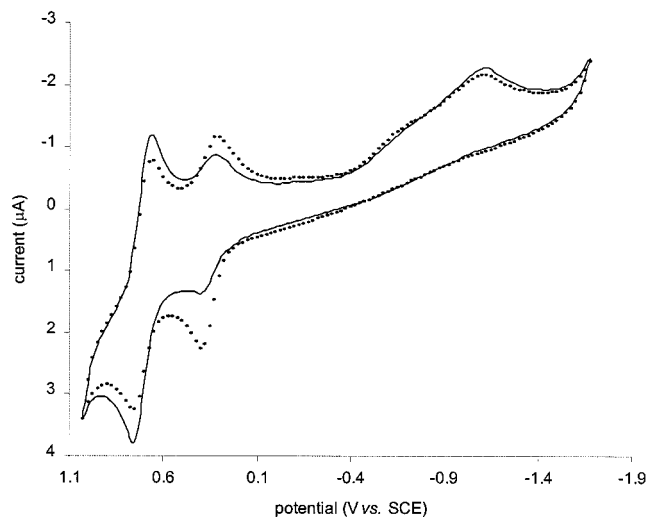
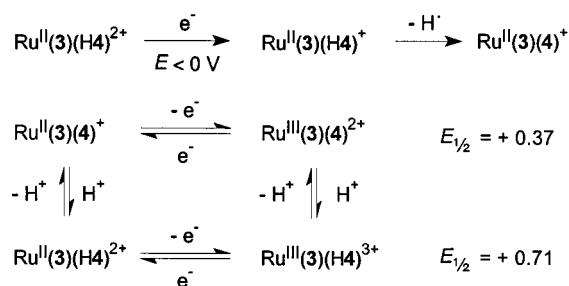


Figure 1. CV of $[\text{Ru}(\mathbf{3})(\text{H4})](\text{PF}_6)_2$ in CH_2Cl_2 showing initial (full line) and steady-state (dotted line) full scans.

Scheme 3



at +0.37 V. There were also cathodic peaks near -0.65 and -1.1 V (Figure 1). Haga described pH-dependent variations in oxidation wave intensity ratios for Ru^{II} complexes of benzimidazoles and attributed the different waves to different protonation states,²⁵ and it is reasonable to analogously attribute the wave at +0.71 V to a standard $[\text{Ru}(\mathbf{3})(\text{H4})]^{3+/2+}$ couple and that at +0.37 V to the analogous process with the deprotonated form, i.e. $[\text{Ru}(\mathbf{3})(\mathbf{4})]^{2+/+}$, undergoing slow proton exchange.

If the sample was not scanned to negative potentials, the intensities of the two oxidation waves were stable but, upon cycling to negative potentials, the more positive wave decreased in intensity while that at +0.37 V increased (Figure 1). Hage et al. witnessed a similar phenomenon with $[\text{Ru}(\text{bpy})_2(\text{HL})]^{2+}$ species where HL is an *N*-H-bearing triazolylpyridine:²² after cycling negative through the reduction wave, a second, less positive oxidation wave appeared and became dominant. These authors explained that the reduced form $[\text{Ru}^{\text{II}}(\text{bpy})_2(\text{HL}^{\bullet-})]^+$ lost H^+ but did not explain how the product, $[\text{Ru}^{\text{II}}(\text{bpy})_2(\text{L}^{\bullet 2-})]^0$, was reoxidized to $[\text{Ru}^{\text{II}}(\text{bpy})_2(\text{L}^-)]^+$ before further oxidation to $[\text{Ru}^{\text{III}}(\text{bpy})_2(\text{L}^-)]^{2+}$ at the new oxidation wave. The reoxidation of $[\text{Ru}^{\text{II}}(\text{bpy})_2(\text{L}^{\bullet 2-})]^0$ should have occurred at a less negative potential than the corresponding reoxidation of $[\text{Ru}^{\text{II}}(\text{bpy})_2(\text{HL}^{\bullet-})]^+$. Further, it is counterintuitive that H^+ should be lost upon reduction when the oxidized forms should be stronger acids. In the present case, we reason that scanning negative caused a change in the intensity ratio by effecting a shift in the H^+ mass balance: a shift toward the deprotonated form indicates a net loss of H^+ , which can be rationalized, as in Scheme 3, by loss of H^+ upon reduction of ligated H4. The product $[\text{Ru}^{\text{II}}(\mathbf{3})(\mathbf{4})]^+$ is reoxidized only at +0.37 V.

Similar but more complicated events occurred with $[\text{Ru}(\text{H}_2\mathbf{2})]^{2+}$ in DMSO. CV revealed a major, well-defined oxidation wave at +0.63 V vs SCE with three smaller waves at +0.46, +0.10 and -0.21 V vs SCE and an initial cathodic peak current ratio of about 6.9:2.8:2.0:1.5. No distinct reduction wave was detected to the negative potential limit (-1.49 V). On the anodic scan, the intensities of the two most positive waves decreased while those of the two least positive waves increased. This continued upon repeated cycling until a fairly stable cathodic current ratio of 4.1:2.4:2.4:2.1 was achieved. If, in analogy to the previous case, H^+ was lost at negative potentials, then, unlike the previous, heteroleptic case, no reoxidation peak was expected and none was seen.

Supramolecular Interactions. When $[\text{Ru}(\text{H}_2\mathbf{13})_2](\text{PF}_6)_2$ in CH_3CN was treated with aliquots of Et_3N (up to 5 equiv), no change was seen in the UV–visible spectra but the ^1H NMR signals in CD_3CN were strongly broadened and new broad signals appeared. We suspect that deprotonated forms acted as counterions in supramolecular assemblies that, because of the increased mass, suffered faster relaxation and line broadening. A literature report of supramolecular H bonding between dicarboxylate ions and a Ru^{II} terpyridine complex bearing thioureido side chains also cites pronounced line broadening with little change in the positions of the terpyridine NMR signals.¹⁹ Pronounced broadening was also observed with the PF_6^- salt of methyl viologen (MV^{2+}) in the presence of Et_3N , though there was no sign of the cation radical ($\lambda_{\text{max}} 607$, $\epsilon 13\,900 \text{ M}^{-1} \text{ cm}^{-1}$).²⁶ This may have been due to $\text{PF}_6^-/\text{OH}^-$ exchange arising from traces of water. When a mixture of $[\text{Ru}(\text{H}_2\mathbf{13})_2](\text{PF}_6)_2$ and $\text{MV}(\text{PF}_6)_2$ was similarly titrated, there were no detectable spectral changes absent with the controls, but >2 equiv of Et_3N produced a precipitate from CH_3CN and the supernatant was depleted of the Ru complex. The isolated red solid was insoluble in organic solvents. Its ^1H NMR spectrum in D_2O , which is expected to destroy any supramolecular association, showed signals for the intact Ru species and MV^{2+} in a reproducible 2:1 molar ratio, indicating that the precipitation was of a salt of formulation $(\text{MV})[\text{Ru}(\text{H}\mathbf{13})(\mathbf{13})_2]$ (Figure 2). Unfortunately, all attempts at recrystallizing this precipitate from H_2O produced powders, but further characterization is underway.

In contrast, analogous titrations with $[\text{Ru}(\text{H}_2\mathbf{2})_2](\text{PF}_6)_2$ produced no precipitate and the resulting spectra were the simple superpositions of the control spectra. We conclude that the deprotonated forms of $[\text{Ru}(\text{H}_2\mathbf{2})_2](\text{PF}_6)_2$ do not engage in significant interactions with MV^{2+} .

Experimental Section

General. $\text{Ru}(\text{DMSO})_4\text{Cl}_2$ was prepared by a literature method.¹⁵ Anhydrous ethylene glycol and DMF were from Aldrich. THF was distilled over K and benzophenone. DMSO was dried (CaO) and distilled over molecular sieves (5 Å) and was then frozen and stored in sealed vials under Ar. Other solvents were reagent grade and used without drying or purification. The petroleum ether (PE) used was the light fraction (bp 30–60 °C). Cyclic voltammetry (CV) was performed using a Pine Instruments RDE-3 potentiostat. A conventional three-electrode cell was used in all experiments. The working electrode was a Pt disk (0.196 mm²), and the quasi-reference electrode was Ag/AgCl wire. A Pt wire was used as a counter electrode. Ferrocene was added at the end of each experiment, and its reference potential was taken as +0.450 V vs SCE in CH_2Cl_2 and +0.50 V vs SCE in DMSO.²⁷ UV–visible spectra were recorded with a Hewlett-Packard 8452A diode array spectrophotometer. NMR spectra were obtained on a 400-MHz Bruker AMX instrument in CD_3CN , unless otherwise indicated. Mass spec-

(25) Haga, M.-A. *Inorg. Chim. Acta* **1983**, 75, 29.

(26) Watanabe, T.; Honda, K. *J. Phys. Chem.* **1982**, 86, 2617.

(27) Lever, A. B. P. *Inorg. Chem.* **1978**, 17, 1146.

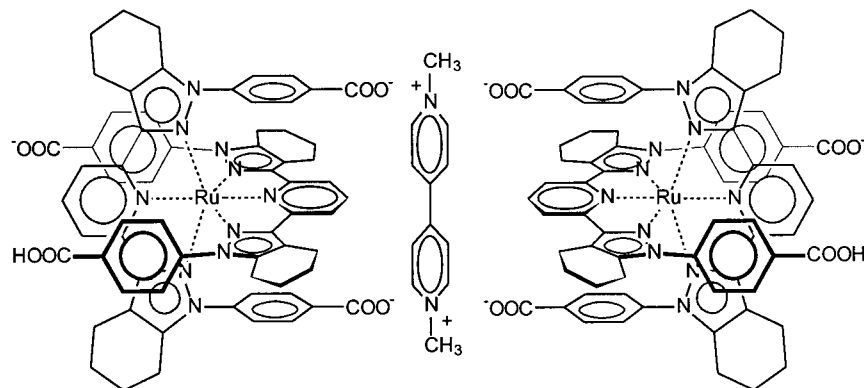


Figure 2. Proposed salt of formulation (MV)[Ru(H13)(13)]₂.

trosopy was carried out in FAB mode by Dr. B. Khouw on a Kratos Profile machine. Peak intensities are reported as a percentage of the base peak intensity. Microanalyses were performed by Guelph Chemical Laboratories Ltd. (Guelph, ON), National Chemical Consulting Inc. (Tenafly, NJ), or Canadian Microanalytical Services (Delta, BC).

Method A: Synthesis of [Ru(H₂)₂](PF₆)₂. A mixture of H₂2 (0.783 g, 2.45 mmol) and Ru(DMSO)₄Cl₂ (0.595 g, 1.225 mmol) was heated to reflux under Ar in 20 mL of anhydrous ethylene glycol for 3 days. After cooling, the reaction mixture was treated with an aqueous solution containing a slight excess of NH₄PF₆ (0.408 g, 2.5 mmol) and stirred for 20 min. An orange-red precipitate formed instantaneously. After cooling in the refrigerator for 1 h, filtration and vacuum-drying produced the red [Ru(H₂)₂](PF₆)₂ in quantitative yield. Its spectra were identical to those of the Cl⁻ salt previously reported.⁷ Anal. Calcd for C₃₈H₄₂N₁₀P₂F₁₂Ru·2H₂O: C, 42.82; H, 4.35; N, 13.14. Found: C, 42.96; H, 3.97; N, 13.14.

Method A': Synthesis of [Ru(5)₂](PF₆)₂. Method A was first followed, using diester **5** (0.205 g, 0.33 mmol) and Ru(DMSO)₄Cl₂ (0.080 g, 0.165 mmol). The reaction mixture was treated with aqueous saturated solution of NaCl and extracted into CHCl₃. After removal of the solvent, the dark-red oil was vacuum-dried and was then redissolved in 20 mL EtOH and treated with DBU (0.100 g, 0.66 mmol) and LiCl (0.140 g, 3.3 mmol). After 48 h at reflux, the EtOH was removed and the remaining yellow oil was triturated with dilute HCl and extracted into CHCl₃. Removal of the solvent afforded a red solid, Ru(5)₂Cl₂, which was purified by column chromatography on silica gel, using CHCl₃/MeOH (90:10) as eluent. After collecting the appropriate fractions and liberating them of solvents, the red solid residue was dissolved in MeOH and treated with excess NH₄PF₆ in H₂O to produce the brick-red Ru(5)₂(PF₆)₂ (0.224 g, 84%). ¹H NMR (acetone-*d*₆): δ 1.48 (t, 12H, *J* = 7.0 Hz), 1.80 (m, 8H), 1.94 (m, 8H), 2.32 (m, 8H), 3.03 (m, 8H), 4.48 (q, 8H, *J* = 7.0 Hz), 6.84 (d, 8H, *J* = 8.0 Hz), 7.51 (d, 4H, *J* = 7.0 Hz), 7.59 (t, 2H, *J* = 7.2 Hz), 7.72 (d, 8H, *J* = 8.0 Hz) ppm. ¹³C NMR: δ 14.54, 21.42, 22.08, 22.50, 62.42, 118.92, 120.38, 127.30, 130.80, 133.36, 136.28, 139.46, 147.57, 151.92, 154.32, 157.68, 162.05, 165.70, 168.80 ppm. MS *m/z* (%) 1622 (4, M), 1477 (100, M - PF₆), 1332 (50, M - 2PF₆), 666 (57, (M - 2PF₆)/2). Anal. Calcd for C₇₄H₇₄N₁₀O₈P₂F₁₂Ru·2H₂O: C, 53.59; H, 4.74; N, 8.45. Found: C, 53.73; H, 4.59; N, 8.50.

Method B: Synthesis of [Ru(3)](PF₆)₂. Solid NaH (0.019 g, 0.8 mmol) was added to a solution of Ru(H₂)₂(PF₆)₂ (0.103 g, 0.1 mmol) in dry THF. H₂ evolution was immediate and the solution turned green. The mixture was kept under Ar for 2 h and was then treated with CH₃I (0.071 g, 0.5 mmol) and brought to reflux for 24 h, during which time the color gradually changed to red. After the THF was removed, the red solid residue was dissolved in CHCl₃ and washed with H₂O. The organic layer was evaporated and the solid red residue was chromatographed on alumina, using CH₂Cl₂-MeOH (90:10) as eluent, then reprecipitated as its solid red PF₆⁻ salt as in method A. Yield 0.100 g (92%). The mp and NMR spectra were identical to those reported for material prepared by method A.¹⁸

Method C: Synthesis of [Ru(H₂13)₂](PF₆)₂. A solution of Ru(5)₂Cl₂ (0.014 g, 0.001 mmol) in 5 mL of THF was treated with 2 drops of H₂O, DBU (0.001 g, 0.007 mmol), and LiCl (0.002 g, 0.047 mmol)

and allowed to stand for 4 h. A red precipitate formed and the solution became clear. The precipitate was filtered off and washed with CHCl₃, H₂O, and Et₂O. This provided Ru(H₂13)₂Cl₂ in quantitative yield. Additional purification was carried out by anion exchange as described in method A. ¹H NMR (DMSO-*d*₆): δ 1.73 (m, 8H), 1.86 (m, 8H), 2.24 (m, 8H), 2.24 (m, 8H), 2.87 (m, 8H), 6.68 (d, 8H, *J* = 7.59 Hz), 7.34 (m, 12H), 7.55 (d, 8H, *J* = 7.56 Hz) ppm. ¹³C NMR (DMSO-*d*₆): δ 20.28, 21.09, 21.38, 21.53, 117.45, 119.23, 126.44, 129.72, 132.67, 134.96, 137.96, 146.10, 150.54, 152.75, 166.12 ppm. MS *m/z* (%) 1365 (20, M - PF₆), 1220 (100, M - 2PF₆), 610 (37, (M - 2PF₆)/2). Anal. Calcd for C₆₆H₅₈N₁₀O₈P₂F₁₂Ru: C, 52.49; H, 3.87; N, 9.27. Found: C, 54.88; H, 4.30; N, 9.51.

Ru(3)Cl₃. In a modification of the procedure of Hadda et al.,¹⁶ ligand **3** (0.70 g, 2.01 mol) and RuCl₃ hydrate (0.416 g, 2.01 mol) were dissolved in 35 mL of absolute EtOH and heated to reflux overnight. After removal of solvent, the crude residue was washed with H₂O and extracted into CHCl₃. The CHCl₃ phase was washed with H₂O several times to remove purple and green impurities, leaving a dark brown solution. After removing the CHCl₃, the residue was redissolved in acetone and treated with Et₂O. The dark brown precipitate was vacuum-dried, leaving 0.78 g of Ru(3)Cl₃ (70%). MS *m/z* (%) 519 (1, M - Cl), 483 (10, M - 2Cl). Anal. Calcd for C₂₁H₂₅N₃Cl₃Ru: C, 45.46; H, 4.54; N, 12.62. Found: C, 45.36; H, 4.33; N, 12.45.

[Ru(H₄)₂](PF₆)₂. This was prepared by method A, using 0.034 g of H₄ (0.102 mmol) and 0.025 g of Ru(DMSO)₄Cl₂ (0.051 mmol) and heating for 2 days. The crude, red oily product was purified by column chromatography on silica gel, using MeOH-CH₂Cl₂ (15:85) as eluent, to provide 0.035 g of red solid [Ru(H₄)₂](PF₆)₂ (82%). Anion exchange provided [Ru(H₄)₂](PF₆)₂ in quantitative yield. ¹H NMR (CDCl₃): δ 1.71 (m, 4H), 1.80 (m, 12H), 2.45 (m, 4H), 2.52 (m, 2H), 2.57 (m, 2H), 2.71 (s, 6H), 2.85 (m, 4H), 2.97 (m, 2H), 3.10 (m, 2H), 7.92 (d, 2H, *J* = 7.8 Hz), 7.98 (d, 2H, *J* = 7.9 Hz), 8.08 (t, 2H, *J* = 7.87 Hz), 10.23 (s, 2H) ppm. ¹³C NMR (CDCl₃): δ 20.58, 21.03, 21.44, 21.52, 21.65, 21.89, 22.17, 33.92, 116.73, 118.25, 119.08, 120.02, 136.67, 143.03, 144.80, 149.45, 149.82, 153.75, 154.23 ppm. MS *m/z* (%) 912 (18, M - PF₆ - H), 767 (100, M - 2PF₆ - 2H). Anal. Calcd for C₄₀H₄₆N₁₀P₂F₁₂Ru·H₂O: C, 44.66; H, 4.50; N, 13.02. Found: C, 44.77; H, 4.37; N, 12.75.

[Ru(3)(H₄)]Cl₂ and [Ru(3)(H₄)](PF₆)₂. By method A, Ru(3)Cl₃ (0.100 g, 0.18 mmol) and ligand H₄ (0.060 g, 0.18 mmol) were allowed to react for 3 days. Column chromatography on silica gel, using MeOH-CH₂Cl₂ (15:85) as eluent, provided 0.085 g of the red solid [Ru(3)(H₄)]Cl₂ (55%). ¹H NMR: δ 1.72 (m, 16H), 2.49 (m, 8H), 2.65 (s, 6H), 2.69 (s, 3H), 8.01 (m, 4H), 8.09 (m, 2H) ppm. ¹³C NMR: δ 21.40, 22.11, 22.22, 22.29, 22.65, 23.26, 23.85, 34.37, 34.72, 118.50, 119.59, 120.39, 136.97, 137.16, 144.48, 149.76, 150.31, 154.77, 155.06, 155.87 ppm. MS *m/z* (%) 817 (4, M - Cl), 781 (100, M - 2Cl), 391 (5, (M - 2Cl)/2). Subsequently, [Ru(3)(H₄)](PF₆)₂ was obtained as a red solid in quantitative yield. ¹H NMR: δ 1.81 (m, 16H), 2.50 (m, 8H), 2.64 (s, 6H), 2.69 (s, 3H), 2.98 (m, 8H), 8.11 (m, 4H), 8.19 (m, 2H), 10.81 (s, 1H) ppm. ¹³C NMR: δ 21.06, 21.41, 22.11, 22.60, 23.26, 23.85, 34.53, 34.85, 119.02, 120.33, 120.70, 137.16, 137.58, 144.68, 145.05, 149.57, 150.53, 154.95, 155.27 ppm. MS *m/z* (%) 926 (36, M - PF₆ - H), 779 (100, M - 2PF₆ - 2H). Anal. Calcd for

$C_{41}H_{48}N_{10}P_2F_{12}Ru \cdot H_2O$: C, 45.18; H, 4.62; N, 12.85. Found: C, 45.13; H, 4.58; N, 12.74.

[Ru(3)(5)]Cl₂ and [Ru(3)(5)](PF₆)₂. Using method A', Ru(3)Cl₃ (0.055 g, 0.1 mmol) and diester **5** (0.062 g, 0.1 mmol) were heated to reflux for 3 d. Retro-transesterification was followed by column chromatography on silica gel, using MeOH–CH₂Cl₂ (15:85) as eluent, yielding 0.065 g of pure, red [Ru(3)(5)]Cl₂ (57%). ¹H NMR (CDCl₃): δ 1.47 (t, 6H, *J* = 7.16 Hz), 1.59 (m, 4H), 1.88 (m, 12H), 2.13 (m, 4H), 2.64 (m, 4H), 2.79 (m, 4H), 2.83 (s, 6H), 3.06 (m, 4H), 4.46 (q, 4H, *J* = 7.17 Hz), 6.45 (d, 4H, *J* = 8.19 Hz), 6.96 (d, 2H, *J* = 7.81 Hz), 7.17 (t, 1H, *J* = 7.83 Hz), 7.53 (d, 4H, *J* = 8.12 Hz), 8.15 (m, 3H) ppm. ¹³C NMR (CDCl₃): δ 14.43, 20.07, 21.01, 21.35, 21.43, 21.54, 21.95, 34.26, 61.69, 117.14, 117.22, 118.80, 119.94, 121.49, 126.92, 129.88, 132.29, 136.73, 138.87, 145.46, 147.37, 148.56, 149.84, 154.15, 154.38, 165.05 ppm. This was further characterized as [Ru(3)(5)](PF₆)₂. MS *m/z* (%) 1354 (8, M), 1208 (100, M – PF₆ – H), 1062 (25, M – 2PF₆ – 2H). Anal. Calcd for C₅₈H₆₂N₁₀O₄P₂F₁₂Ru · 0.5H₂O: C, 51.10; H, 4.66; N, 10.27. Found: C, 51.02; H, 4.56; N, 10.08.

[(3Ru)₂12](PF₆)₄. Ditopic ligand **12** (0.215 g, 0.317 mmol) and Ru(3)Cl₃ (0.352 g, 0.634 mmol) in 15 mL of ethylene glycol were heated at 140° for 5 days. The reaction mixture was treated with saturated aqueous NaCl and extracted with CHCl₃. An insoluble red film was observed on the walls of the separatory funnel. The CHCl₃ layer was separated, the solvent was removed, the residue was dissolved in MeOH, and the crude product was precipitated as its PF₆[–] salt as before. The red film was dissolved in MeOH and separately treated with NH₄PF₆ as before. The red solids so obtained were washed with H₂O and purified by chromatography on silica gel, using 1:9 MeOH–CH₂Cl₂ as eluent. This produced 0.307 g (45%) of the binuclear complex which was recrystallized from acetone–H₂O. ¹H NMR: δ 0.25 (m, 2H), 0.54 (m, 2H), 0.93 (m, 4H), 1.30 (m, 6H), 1.36 (m, 4H), 1.76 (m, 8H), 2.40 (s, 6H), 2.42 (m, 6H), 2.51 (m, 6H), 2.55 (m, 4H), 2.59 (s, 6H), 2.72 (s, 6H), 2.75 (m, 4H), 3.00 (m, 2H), 3.15 (m, 2H), 3.30 (m, 2H), 4.19 (s, 2H), 7.87 (d, 2H, *J* = 8.12 Hz), 7.97 (t, 2H, *J* = 7.92 Hz), 8.15 (m, 6H), 8.24 (t, 2H, *J* = 7.90 Hz) ppm. ¹³C NMR: δ 20.00, 21.34, 21.88, 22.16, 22.49, 22.80, 33.82, 34.56, 34.77, 62.26, 118.63, 119.06, 119.77, 121.26, 121.52, 121.73, 122.18, 137.94, 138.13, 145.61, 145.71, 145.90, 146.09, 149.20, 149.47, 149.76, 151.15, 154.70, 155.13, 155.23 ppm. MS *m/z* (%) 2010 (1, M – PF₆ – H), 780 (10, [Ru(3)(4)]⁺). Anal. Calcd for C₈₃H₉₆N₂₀P₄F₂₄Ru₂ · CH₃COCH₃ · H₂O: C, 46.28; H, 4.70; N, 12.55. Found: C, 46.21; H, 4.69; N, 12.32.

[Ru(H6)](PF₆)₂. Method A' was followed, using monoester **H6** (0.072 g, 0.154 mmol), Ru(DMSO)₄Cl₂ (0.037 g, 0.077 mmol) and heating to reflux for 3 days. After transesterification, column chromatography on silica gel, using MeOH–CH₂Cl₂ (10:90), and anion exchange provided pure red [Ru(H6)](PF₆)₂ (0.033 g, 33%). ¹H NMR: δ 1.55 (t, 6H, *J* = 6.96 Hz), 1.76 (m, 8H), 1.85 (m, 4H), 1.93 (m, 4H), 2.23 (m, 2H), 2.48 (m, 6H), 2.89 (m, 6H), 3.02 (m, 2H), 4.53 (q, 4H, *J* = 6.97 Hz), 6.36 (m, 2H), 6.71 (m, 2H), 7.58 (m, 4H), 7.87 (m, 6H) ppm. ¹³C NMR: δ 14.61, 21.37, 21.47, 22.14, 22.30, 22.61, 22.83, 62.45, 118.68, 118.80, 120.10, 120.15, 127.42, 130.52, 133.31, 136.58, 139.66, 144.96, 146.04, 150.48, 151.68, 153.90, 154.69, 165.70 ppm. MS *m/z* (%) 1181 (9, M – PF₆), 1036 (100, M – 2PF₆), 518 (42, M – 2PF₆)/2). Anal. Calcd for C₅₆H₅₈N₁₀O₄P₂F₁₂Ru · 2C₂H₆O: C, 54.88; H, 4.84; N, 9.89. Found: C, 50.75; H, 4.65; N, 9.93.

[Ru(7)₂](PF₆)₂. Method B was followed, using 0.019 g of NaH (0.8 mmol), 0.103 g of Ru(H₂)₂(PF₆)₂ (0.1 mmol), and 10 mL of EtBr, and heating to reflux for 24 h. Anion exchange as before afforded [Ru(7)₂](PF₆)₂ in quantitative yield. ¹H NMR (acetone-*d*₆): δ 0.54 (t, 12H, *J* = 7.02 Hz), 1.82 (m, 16H), 2.63 (m, 8H), 3.09 (m, 8H), 3.24 (q, 8H, *J* = 7.47 Hz), 8.37 (d, 4H, *J* = 7.88 Hz), 8.46 (t, 2H, *J* = 7.38 Hz) ppm. ¹³C NMR: δ 15.19, 21.42, 21.88, 22.11, 22.45, 44.72, 119.57, 120.65, 138.41, 145.07, 149.96, 155.58 ppm. MS *m/z* (%) 996 (100, M – H – PF₆), 850 (27, M – 2H – 2PF₆). Anal. Calcd for C₄₆H₅₈N₁₀P₂F₁₂Ru: C, 48.38; H, 5.12; N, 12.26. Found: C, 48.00; H, 5.10; N, 12.13.

[Ru(8)₂](PF₆)₂. By Method B, 0.020 g of NaH (0.8 mmol), 0.103 g of Ru(H₂)₂(PF₆)₂ (0.1 mmol), and 0.086 g of benzyl bromide (0.5 mmol) were used with overnight heating at reflux. Purification was carried out by column chromatography on silica gel, using first MeOH–

CH₂Cl₂ (5:95) to remove the unreacted benzyl bromide then MeOH–CH₂Cl₂ (10:90) to collect [Ru(8)₂]Cl₂, followed by anion exchange as before to give 0.120 g (86%) of red solid. ¹H NMR: δ 1.72 (m, 16H), 2.27 (m, 8H), 2.57 (m, 8H), 4.28 (s, 8H), 5.91 (d, 8H, *J* = 7.40 Hz), 7.04 (t, 8H, *J* = 7.62 Hz), 7.21 (t, 4H, *J* = 7.26 Hz), 7.63 (d, 4H, *J* = 7.94 Hz), 8.03 (t, 2H, *J* = 7.91 Hz) ppm. ¹³C NMR: δ 21.31, 21.71, 22.38, 24.79, 51.45, 119.40, 120.94, 124.53, 128.35, 129.26, 135.46, 137.50, 145.94, 150.32, 154.81 ppm. MS *m/z* (%) 1244 (100, M – H – PF₆), 1100 (30, M – 2PF₆), 550 (40, M – 2PF₆)/2). Anal. Calcd for C₆₆H₆₆N₁₀P₂F₁₂Ru: C, 57.02; H, 4.78; N, 10.07. Found: C, 57.36; H, 4.50; N, 9.70.

[Ru(9)₂](PF₆)₂. Method B was followed, using 0.024 g of NaH (1.0 mmol), 0.120 g of Ru(H₂)₂(PF₆)₂ (0.12 mmol), and 0.260 g of methyl 4-(bromomethyl)benzoate (1.13 mmol), and heating at reflux for 48 h. Purification consisted of washing the crude chloride salt with Et₂O and precipitation of the PF₆[–] salt as before. This yielded 0.190 g of the red [Ru(9)₂](PF₆)₂ (98%). ¹H NMR: δ 1.67 (m, 16H), 2.27 (m, 8H), 2.48 (m, 8H), 3.89 (s, 12H), 4.33 (s, 8H), 6.02 (d, 8H, *J* = 8.02 Hz), 7.60 (d, 4H, *J* = 7.98 Hz), 7.66 (d, 8H, *J* = 8.37 Hz), 8.04 (t, 2H, 7.65 Hz) ppm. ¹³C NMR: δ 21.24, 21.67, 22.10, 51.48, 52.73, 119.49, 121.35, 124.92, 130.29, 130.33, 137.89, 140.59, 146.35, 150.50, 154.61, 167.02 ppm. MS *m/z* (%) 1476 (100, M – H – PF₆), 1330 (71, M – 2H – 2PF₆), 665 (85, M – 2H – 2PF₆)/2). Anal. Calcd for C₇₄H₇₄N₁₀O₈P₂F₁₂Ru: C, 54.73; H, 4.60; N, 8.63. Found: C, 56.66; H, 4.71; N, 7.37.

[Ru(10)₂](PF₆)₂. Following method B, 7 mg of NaH (0.3 mmol), 0.052 g of Ru(H₂)₂(PF₆)₂ (0.050 mmol), and 0.043 g of ethyl iodoacetate (0.20 mmol) were used with 24 h heating at reflux. Column chromatography on silica gel using MeOH–CH₂Cl₂ (10:90) and anion exchange as before yielded red [Ru(10)₂](PF₆)₂, which was recrystallized from acetone–H₂O (0.056 g, 81%). ¹H NMR: δ 1.14 (t, 12H, *J* = 7.1 Hz), 1.83 (m, 16H), 2.44 (m, 8H), 2.98 (m, 8H), 3.78 (s, 8H), 3.85 (q, 8H, *J* = 6.99 Hz), 8.01 (d, 4H, *J* = 7.98 Hz), 8.16 (t, 2H, *J* = 7.95 Hz) ppm. ¹³C NMR: δ 13.88, 21.22, 21.69, 48.94, 61.81, 118.44, 119.68, 136.83, 146.40, 148.92, 154.62, 165.40 ppm. MS *m/z* (%) 1228 (100, M – H – PF₆), 1082 (35, M – 2H – 2PF₆), 541 (47, M – 2H – 2PF₆)/2). Anal. Calcd for C₅₄H₆₆N₁₀O₈P₂F₁₂Ru · H₂O · CH₃COCH₃: C, 47.21; H, 5.14; N, 9.66. Found: C, 47.14; H, 4.91; N, 9.36.

[Ru(11)₂](PF₆)₂. Using method B, with 0.066 g of [Ru(H₄)₂](PF₆)₂ (0.06 mmol), 0.005 g of NaH (0.21 mmol) in 25 mL of CH₂Br₂ was heated at reflux for 24 h. The removal of solvent and subsequent washing of the product with CHCl₃/H₂O gave a dark red solid, which was purified by silica gel chromatography, using CH₂Cl₂–MeOH (95:5) as eluent, followed by anion exchange to give [Ru(11)₂](PF₆)₂ as a red solid (0.058 g, 78%). ¹H NMR (35 mg/mL): δ 1.81 (m, 16H), 2.48 (m, 4H), 2.56 (m, 4H), 2.63 (s, 6H), 2.98 (m, 8H), 4.71 (d, 2H, *J* = 11.0 Hz), 4.85 (d, 2H, *J* = 11.0 Hz), 8.35 (m, 6H) ppm. ¹³C NMR: δ 21.39, 21.76, 22.15, 22.53, 34.42, 41.62, 119.39, 121.41, 121.70, 122.11, 138.46, 145.90, 146.68, 150.07, 153.61, 154.92, 155.74 ppm. MS *m/z* (%) 1096 (24, M – 2PF₆ – 2H). Anal. Calcd for C₄₂H₄₈N₁₀Br₂P₂F₁₂Ru · 1/2 C₄H₁₀O: C, 41.26; H, 4.17; N, 10.94. Found: C, 41.03; H, 4.39; N, 10.86.

[Ru(H₂14)₂](PF₆)₂. By method C, using 0.051 g of [Ru(9)₂](PF₆)₂ (0.031 mmol) in THF and a mixture of LiCl (0.026 g, 0.62 mmol), DBU (0.049 g, 0.32 mmol), and H₂O (0.100 g) in 4 mL of THF, were heated at reflux for 4 days. After removal of THF, the oily residue was dissolved in H₂O and acidified with dilute HCl. The dark red solid formed was collected, redissolved in MeOH–H₂O, and subjected to anion exchange as before. The PF₆[–] salt was washed with H₂O and CHCl₃, then vacuum-dried to yield 0.036 g of the red [Ru(H₂14)₂](PF₆)₂ (74%). ¹H NMR (DMSO-*d*₆): δ 1.60 (m, 16H), 2.27 (m, 8H), 2.44 (m, 8H), 4.42 (s, 8H), 5.95 (d, 8H, *J* = 7.86 Hz), 7.63 (d, 8H, *J* = 7.91 Hz), 7.89 (d, 4H, *J* = 7.54 Hz), 8.21 (t, 2H, *J* = 7.80 Hz) ppm. ¹³C NMR (DMSO-*d*₆): δ 20.22, 20.48, 21.09, 21.34, 21.80, 22.46, 50.32, 117.96, 120.46, 123.56, 129.48, 130.32, 137.60, 139.05, 145.08, 149.00, 153.18, 166.94 ppm. MS *m/z* (%) 1512 (21, M – CO₂), 1421 (96, M – PF₆), 1276 (60, M – 2PF₆), 1231 (34, M – 2PF₆ – CO₂), 1141 (100, M – 2PF₆ – 3CO₂). Anal. Calcd for C₇₀H₆₆N₁₀O₈P₂F₁₂Ru: C, 53.68; H, 4.25; N, 8.94. Found: C, 56.53; H, 4.66; N, 8.25.

[Ru(H₂15)₂](PF₆)₂. Ru(10)₂(PF₆)₂ (0.073 g, 0.053 mmol), LiCl (0.045 g, 1.06 mmol), DBU (0.045 g, 1.06 mmol) and H₂O (0.1 g) were used in THF (25 mL) at reflux for 3 days, according to method C. The THF

was removed, the residue was taken up in H₂O and this was acidified with HCl. The dark red precipitate was collected, redissolved in MeOH-H₂O, and subjected to anion exchange as before. The red PF₆⁻ salt was vacuum-dried to yield 0.035 g of [Ru(H₂15)₂](PF₆)₂ (52%). ¹H NMR (CF₃COOD): δ 2.03 (m, 16H), 2.68 (m, 8H), 3.21 (m, 8H), 4.22 (s, 8H), 8.46 (d, 4H, *J* = 7.46 Hz), 8.57 (t, 2H, *J* = 7.8 Hz) ppm. ¹³C NMR (CF₃COOD): δ 22.78, 23.23, 50.26, 122.06, 122.734, 140.94, 150.03, 152.93, 156.88, 173.19 ppm. MS *m/z* (%) 972 (11, M - 2PF₆), 913 (30, M - 2PF₆ - CH₂CO₂H), 854 (26, M - 2PF₆ - 2CH₂CO₂H), 795 (91, M - 2PF₆ - 3CH₂CO₂H). Anal. Calcd for C₄₆H₅₀N₁₀O₈P₂F₁₂-

Ru·6H₂O: C, 40.33; H, 4.56; N, 10.22. Found: C, 40.24; H, 4.52; N, 9.91.

Acknowledgment. The authors are indebted to Mr. Robert Dash for initial work with [Ru(H₂2)₂]²⁺, to Ms. Sundeep Shahi for the experiments with MV(PF₆)₂, to Mr. Mehrdad Ebadi and Prof. A. B. P. Lever for CV runs and discussions, and to the Natural Sciences and Engineering Research Council for funding.

IC980817H